Title
Accurate dispensing of volatile reagents on demand for chemical reactions in EWOD chips

Journal
Lab on a Chip, 12(18)

ISSN
1473-0197

Authors
Ding, Huijiang
Sadeghi, Saman
Shah, Gaurav J
et al.

Publication Date
2012

DOI
10.1039/c2lc40244k

Peer reviewed

Authors' final manuscript for: *Lab Chip*, 2012, 12, 3331–3340

Accurate dispensing of volatile reagents on demand for chemical reactions in EWOD chips

Huijiang Ding[1,2], Saman Sadeghi[1,2], Gaurav J. Shah[1,2,5], Supin Chen[3], Pei Yuin Keng[1,2], Chang-Jin "CJ" Kim[4], R. Michael van Dam[1,2,3]

[1]Crump Institute for Molecular Imaging, [2]Department of Molecular & Medical Pharmacology, [3]Biomedical Engineering Interdepartmental Program, [4]Mechanical and Aerospace Engineering Department, University of California, Los Angeles (UCLA), USA, [5]Sofie Biosciences, Culver City, CA, USA

1 ABSTRACT

Digital microfluidic chips provide a new platform for manipulating chemicals for multi-step chemical synthesis or assays at the microscale. The organic solvents and reagents needed for these applications are often volatile, sensitive to contamination, and wetting, i.e. have contact angles of < 90° even on the highly hydrophobic surfaces (e.g., Teflon® or Cytop®) typically used on digital microfluidic chips. Furthermore, often the applications dictate that the processes are performed in a gas environment, not allowing the use of a filler liquid (e.g., oil). These properties pose challenges for delivering controlled volumes of liquid to the chip. An automated, simple, accurate and reliable method of delivering reagents from sealed, off-chip reservoirs is presented here. This platform overcomes the issues of evaporative losses of volatile solvents, cross-contamination, and flooding of the chip by combining a syringe pump, a simple on-chip liquid detector and a robust interface design. The impedance-based liquid detection requires only minimal added hardware to provide a feedback signal to ensure accurate volumes of volatile solvents are introduced to the chip, independent of time delays between dispensing operations. On-demand dispensing of multiple droplets of acetonitrile, a frequently used but difficult to handle solvent due to its wetting properties and volatility, was demonstrated and used to synthesize the positron emission tomography (PET) probe [^{18}F]FDG reliably.

2 INTRODUCTION

Digital microfluidic devices based on electrowetting-on-dielectric (EWOD) and dielectrophoresis (DEP) electronically manipulate droplets on chip to perform a variety of applications in biology [1][2], biochemistry [3][4][5][6][7] and chemistry [8][9][10]. To automate these applications, reagents and samples can be stored on chip as "reservoir droplets" [11], above the chip in wells [12], or in off-chip locations [13] and dispensed on-demand when they are needed. Automation not only improves user-friendliness and repeatability but can also increase safety in applications dealing with hazardous materials such as radiolabeled tracers for medical imaging [10].

Chemistry applications often require handling of volatile organic solvents in a gaseous environment. Although droplet actuation of a wide variety of solvents on a digital microfluidics device using a combination EWOD and DEP has been experimentally demonstrated [14], [15], the droplets in these reports were manually loaded onto the chip just prior to the actuation. On-chip storage is not possible (unless solvent droplets are sealed individually) due to evaporative losses and the potential for vapor cross-contamination. Furthermore, organic solvents are typically wetting (i.e. have contact angles <90°) even on highly hydrophobic materials such as Cytop® or Teflon® that are typically used on the surfaces of digital microfluidic chips. If stored in wells above the chip, the wetting organic solvents would flood the chip spontaneously, unlike the usual non-wetting aqueous liquids that are repelled from the chip [16]. Storage of reagents in off-chip reservoirs can address all of these concerns. A pneumatically-driven system for *continuous* droplet-generation from a sealed off-chip reservoir has been reported for aqueous solutions [13]; however, this approach does not appear to have sufficient control for on-demand delivery, particularly in the case of wetting liquids. We have demonstrated on-demand delivery of non-aqueous reagents using a combination

of pneumatics, gravity and EWOD actuation [16], but the volume loaded was dictated by the EWOD electrode size and could not be fine-tuned.

Here we demonstrate a syringe pump-based system to deliver precise and controllable volumes of volatile reagents on demand. The use of a closed pump provides a holding force that prevents uncontrollable flooding of the chip, even when the liquid contacts the chip, while also protecting sensitive reagents from environmental contamination until they are needed. Though syringe pumps are capable of dispensing accurate volumes, there is significant evaporation of volatile liquids from the open end of the dispensing interface, and compensation is required to ensure high accuracy of delivered volumes after arbitrary delays. This compensation is provided by using on-chip impedance sensing to create a very sensitive liquid detector using only minimal hardware beyond what is normally needed for EWOD actuation [17][18]. With our particular configuration, evaporative losses are compensated with a resolution of about 2 nL.

We demonstrate the use of this interface to load the volatile solvent acetonitrile (MeCN) for several steps of the radiochemical synthesis of 2-[^{18}F]fluoro-2-deoxy-D-glucose ([^{18}F]FDG), a molecular probe used in positron emission tomography [19] for diagnosis of cancer [20], searching for metastases [21], monitoring response to therapy [22] and drug development [23]. Automation of reagent dispensing is particularly important in this application due to the need to shield the operator from radiation emitted by the starting materials and synthesized probe as well as the requirement for multiple precision loadings of the solvent at various stages of the reaction.

3 Experimental

3.1 Fabrication of EWOD Chip

The bottom substrate of the parallel-plate EWOD chip was fabricated from a 700 µm thick glass wafer coated with 140 nm indium tin oxide (ITO) (TechGophers Inc., USA). The wafer was first covered with 20 nm of chromium and 200 nm of gold using an e-beam evaporator. Metal and ITO layers were etched to form EWOD electrodes (2 mm x 2 mm), heater electrodes (circular electrode with radius 6mm for application-specific radiosynthesis chip described later), connection lines, and contact pads. 1 µm silicon nitride was coated as a dielectric layer by plasma-enhanced chemical-vapor-deposition (PECVD), and 1 µm of Cytop® was spin-coated and annealed at 200°C to make the surface hydrophobic. A top substrate (cover plate) was prepared from 700 µm thick glass coated with 150 nm ITO (Delta Technologies Inc., USA) to serve as a ground electrode for electrowetting. The cover plate was coated with PECVD silicon nitride (100 nm) and Cytop® (100 nm). One edge of the cover plate was also coated with Cytop® film and served as the reagent-loading edge. The cover plate was affixed to the bottom EWOD substrate with double-sided adhesive (3M Inc., USA) such that the reagent-loading edge was aligned with the edge of the loading electrode on the bottom EWOD substrate. The nominal adhesive thickness (and thus gap height) was 100 µm; however, significant variation was observed and the gap for each chip was measured.

3.2 Actuation of Droplets

A 10 kHz, 0.7 V_{rms} signal, V_{ref}, was generated with a data acquisition (DAQ) module (NI USB-6211, National Instruments, USA) and amplified with a custom-built amplifier to ~100 V_{rms}. The 10 kHz, 100 V_{rms} signal was used to activate EWOD electrodes to transport droplets from the loading interface into the EWOD chip. Individual control of electrodes was achieved using manual switches that connected each electrode to the 100 V_{rms} AC signal or to ground. The ground electrode of the cover plate was connected to the power supply ground.

3.3 Design of Reagent Dispensing System

A schematic of the reagent dispensing system is depicted in **Fig. 1A**. The volatile reagent is first loaded into a syringe pump (PSD4, Hamilton Company, USA) that is connected via a PTFE delivery line (1/32" OD) to the EWOD chip. The delivery line is terminated in the blunt end of a 30G needle (Becton, Dickinson and Co., USA) with the tip positioned adjacent to the gap between the two substrates of the EWOD chip at the loading site. The syringe valve is switched to the dispense position, and the delivery tube is primed by pumping the reagent toward the EWOD chip until all air is eliminated from the tip of the needle. The syringe pump is controlled by a computer to deliver the desired volume of reagent on demand to the EWOD chip.

To prime the delivery line, and to compensate for evaporation loss from the needle interface between dispensing operations, an on-chip liquid detector was implemented based on impedance sensing between the loading electrode (EWOD electrode adjacent the loading site) in the bottom substrate and the ground electrode in the cover plate (**Fig. 1B,C**). To prime the system, the pump is advanced in small increments of 2.1 nL, achieved using a 50 µL syringe with 24000 steps per stroke, until the leading meniscus of the liquid is detected at the chip. Prior to delivery of a droplet, the same action is performed, but is immediately followed by rapid dispensing of the desired reagent volume from the syringe pump. The EWOD chip is then actuated to cut the droplet from the fluid in the needle and transport it to the desired location for processing or analysis.

3.4 Liquid Detection Subsystem

The basic elements of the liquid detection circuit are shown in **Fig. 1A**. A resistor, $R \approx 1$ kΩ, is placed between the ground electrode in the cover plate and the power supply ground. The activation of an EWOD electrode, as discussed above, generates a sinusoidal current and a corresponding voltage drop, V_R, across this resistor, which is sensitive to the impedance between the ground electrode in the cover plate and the (activated) loading electrode in the bottom substrate. Approximated as a parallel-plate capacitor, the impedance is affected by the amount and type of liquid located in the gap. This technique affords real-time pico-liter liquid volume sensing resolution [18] on the EWOD chips used in this paper, effectively eliminating priming error due to liquid detection. A comprehensive theoretical model of the relationship between liquid volume (and other parameters) and V_R is also described in reference [18].

To sense the liquid, the loading electrode is actuated normally and V_R is measured by the DAQ module continuously. Using the phase information from V_{ref}, $\mathrm{Im}\{V_R\}$ is determined and compared to a threshold value to detect the presence or absence of liquid at the electrode site. Threshold detection and control of the syringe pump were integrated into a custom LabView program. The details on the selection of threshold value are discussed in the results. It should be noted that most of the components of this system are part of the existing EWOD actuation platform.

When the operator initiates a droplet dispensing operation, there is a small time delay while the system advances the liquid in increments and monitors the liquid-detection circuitry. After the signal reaches the threshold value, indicating that liquid has reached the chip, the desired volume is dispensed. The delay depends on the extent of evaporation since the last droplet was dispensed. The performance of the detection algorithm was optimized such that during priming, the syringe dispensed one step every 40 ms (i.e. 25 Hz) while monitoring feedback information from the liquid sensing sub-system after each step. With a 2.1 nL syringe pump step size, this corresponds to 53 nL/s rate of volume compensation. For applications requiring faster and/or more consistent response time before the droplet is actually dispensed, the control program can continuously prime the delivery line to compensate for evaporation and always maintain the droplet ready for immediate dispensing.

3.5 Measurement of Droplet Volumes in Chip

To characterize the accuracy of volume dispensing, loaded droplets were transported to an adjacent electrode immediately after dispensing, and an image of the droplet within the EWOD chip was recorded with a CCD camera (DMK 31AU03.AS, The Imaging Source, Germany). The 2D area of the droplet was estimated with the aid of image processing software (Photoshop CS5, Adobe Systems Inc., USA). For the chips used in these characterization experiments, the height of the gap between the bottom EWOD substrate and cover plate was determined to be 100 µm, by measuring the total chip thickness with calipers and subtracting the thicknesses of the bottom substrate and the cover plate. Multiplying the measured gap by estimated 2D area gave an estimate of the droplet volume.

3.6 Radiosynthesis of 2-[^{18}F]fluoro-2-deoxy-D-glucose ([^{18}F]FDG)

As a demonstration, the reagent loading system was used to deliver droplets to the EWOD-based microfluidic radiosynthesizer [10] for the production of the PET tracer [^{18}F]FDG following the synthesis of Hamacher *et al.* [24] adapted for the microscale. The EWOD chip used for the synthesis (**Fig. 2A**) had a gap height of 180 µm, the larger gap allowing slightly larger volumes, and thus enabling larger amounts of radioactivity to be produced.

3.6.1 Reagents

No-carrier-added (n.c.a.) [^{18}F]fluoride ion was obtained from the UCLA Biomedical Cyclotron Facility by irradiation of 97% ^{18}O-enriched water with an 11 MeV proton beam using a Siemens RDS-112 cyclotron. Anhydrous acetonitrile (MeCN), dimethyl sulfoxide (DMSO), Kryptofix $K_{2.2.2}$ (K-222), mannose triflate, potassium carbonate (K_2CO_3), and 1N hydrochloric acid standard solution (HCl) were obtained from Sigma Aldrich and used as received.

3.6.2 Synthesis

The synthesis, shown in the left part of **Fig. 2B** involves activation of the [^{18}F]fluoride by use of the phase transfer catalyst K-222 and exchange from [^{18}O]water to anhydrous MeCN, followed by radiofluorination of mannose triflate to produce the intermediate 2-[^{18}F]fluoro-1,3,4,6-tetra-O-acetyl-D-glucose ([^{18}F]FTAG) and subsequent hydrolysis to yield [^{18}F]FDG.

[^{18}F]fluoride was prepared by mixing with K_2CO_3 and K-222 to create a solution with 18mM K_2CO_3 and 36mM K-222 in MeCN:H_2O (1:1 v/v). Four 1.5 µL droplets of this [^{18}F]fluoride solution, containing a total of 300 µCi [11 MBq] of radioactivity, were sequentially loaded by pipette at loading electrode #1 (**see Fig. 2B**) and transported to the heater electrode. Next, a 2.0 µL droplet of MeCN was loaded by pipette at loading electrode #1 and transported to the heater to rinse any residual radioactivity into the reaction mixture. The solution was dried by heating to 105˚C for 3 min, creating a solid residue containing the activated [^{18}F]fluoride. This whole loading process was repeated a second time to approximately double the amount of radioactivity loaded.

To further dry the [^{18}F]fluoride and remove residual water by azeotropic distillation, seven 1.5 µL droplets of MeCN were sequentially added by the dispensing system at loading electrode #2 and transported to the heater electrode to create a pool of MeCN that completely covered the initial location of dried residue. The heater was then held at 105˚C for 3 min to evaporate the MeCN. This whole drying procedure was repeated three more times.

To carry out the fluorination reaction, two 2.0 µL droplets of 104 mM mannose triflate in DMSO were sequentially loaded by pipette at loading electrode #1, and transported to the dried residue on the heater. This was followed by the addition of nine 1.5 µL MeCN droplets by the dispensing system at loading electrode #2. The combined mixture completely covered the heater electrode, ensuring all the [^{18}F]fluoride residue would be dissolved into it. The reaction was carried out at 120°C for 10 min. During this time, most of the solvent evaporated.

Finally, to accomplish the hydrolysis, five 2.0 µL droplets of a 1:1 (v/v) mixture of 1N HCl and MeCN were loaded by pipette at loading electrode #1, and transported to the heater to completely redissolve the residue containing [^{18}F]FTAG. An additional five 1.5 µL droplets of MeCN were loaded by the dispensing system at loading electrode #2 and also transported to the heater. Loading and transporting the two types of droplets in an alternating fashion was found to improve reliability of droplet transport. The mixture was heated at 95°C for 5 min to complete the hydrolysis reaction.

3.6.3 Analysis of Synthesized Product

After synthesis, the two plates of the EWOD chip were separated, and the crude product droplet was extracted with a glass capillary from the surfaces at the heater electrode site and a small sample was deposited onto a silica TLC plate (JT4449-2, J.T. Baker, USA). The TLC plate was developed in MeCN:H_2O (95:5 v/v), dried, and read with a radio-TLC scanner (MiniGITA Star, Raytest, Germany). The relative area of the peaks was computed to determine the relative abundance of radioactive species. [^{18}F]fluoride, [^{18}F]FTAG, and [^{18}F]FDG have retention factors (R_f values) of 0.0, 1.0, and 0.56, respectively (Supporting Information, **Fig. S2**). The fluorination efficiency of the reaction was estimated by taking the ratio of the peak area of the desired compound divided by the total area of all peaks.

4 Results and Discussion

4.1 Evaporation from Needle

Although the syringe pump used to store and deliver the reagent has a high accuracy, the volatile reagent can suffer substantial evaporation, even from the small 30G needle used here. For a given geometry (e.g. needle size),

the amount of loss depends on the ambient conditions (e.g. temperature, air flow, and partial pressure of solvent vapor in the surrounding environment) and the amount of time elapsed since the last droplet was dispensed. Evaporation causes the meniscus to retract into the needle and, if not compensated, leads to the next dispensed droplet having a less than desired volume (**Fig. 3A**).

To quantify how much evaporation occurred from the end of the needle as a function of time (**Fig. 3C**), we loaded MeCN into the syringe pump and fixed the needle adjacent to a chip with 91 µm gap between plates. MeCN was pumped until it emerged from the needle into the chip. After the MeCN evaporated back to the needle tip, a timer was started. After the desired time t elapsed, a fixed volume V was pumped, causing liquid to enter the chip. The volume that entered the chip (determined from area A in the optical image and gap height d) was subtracted from V to determine the amount of evaporation $V_e = V - Ad$ that had occurred during the time interval. This procedure was repeated for a range of time delays (< 1 min to 90 min) (**Fig. 3B**) representing the anticipated time delays for a wide range of applications, including multi-step chemical synthesis. For example, in the synthesis of the radiotracer [^{18}F]FDG, the time delay between dispensing operations can be seconds (when replenishing MeCN solvent droplets to maintain the liquid state during reaction steps), or several minutes (when adding MeCN droplets for subsequent [^{18}F]fluoride drying steps). Thus the loss of 30-110 nL can be significant compared with the nominal droplet volume of 400 nL.

4.2 Geometry of Loading Site

Reagents were dispensed from a Cytop®-coated needle onto the Cytop®-coated surface of the bottom EWOD substrate at a position adjacent the gap between the bottom EWOD substrate and the smaller cover plate (**Fig. 4A**). The Cytop® coating on the needle ensures that the droplet quickly moves into the EWOD chip (where contact angle is lower due to activation of loading electrode) rather than spreading to the outside surface of the needle. The blunt-end of the needle was positioned at a 45° angle to the surface less than ~100 µm from the edge of the cover plate and less than ~100 µm from the top surface of the bottom EWOD substrate. With this arrangement all relevant solvents for the application of synthesis of [^{18}F]FDG, including MeCN, water, and DMSO entered the chip gap with an identical geometry of loading site while the loading electrode was activated. Furthermore, droplet delivery through the syringe pump prevents spontaneous capillary flow (SCF). SCF can be especially problematic for organic solvents that are partially wetting (with contact angles <90^{o}), and can enter the chip gap without the application of electric potential. However, while dispensing from the needle, any tendency for spontaneous capillary flow from the needle into the chip will be countered by the cohesion of the fluid maintaining a continuous segment of the (incompressible) liquid from the syringe to the outlet of the needle, and the negative pressure generated at the syringe-end of this continuous segment. The volume delivered from the syringe pump can be controlled with high accuracy and when voltage is applied, the electromechanical force would preferentially direct the liquid towards the actuated electrodes, where it is detected by electrical impedance.

Delivering liquid via a needle avoids the need to add complexity to chip fabrication (e.g. hole drilling, precision alignment of cover plate to bottom substrate, etc.) as would be required if traditional fluidic fittings were used. The above parameter values were selected based on a qualitative comparison of several geometries**(Supporting Information, Fig. S1)**. The performance of loading was not found to be sensitive to the angle of the needle, θ. We selected θ=45°, simply because it removes the needle and any holding fixture from the field of view, thus enabling better visibility of the droplets within the EWOD chip. On the other hand, loading was found to depend significantly on the location of the needle tip: the horizontal proximity to the cover plate (d_x) and the vertical proximity to the bottom substrate (d_z). If d_x or d_z is much larger than ~100 µm, the droplet tends not to touch the edge of the cover plate or bottom substrate, respectively. Both situations reduce the repeatability of the reagent loading to the EWOD chip. Setting each dimension at 100 µm was found to be a good compromise of being close enough yet sufficiently far to avoid scratching the EWOD chip surface.

4.3 Quick-connect Needle Interface

To ensure repeatable and rapid setup of needles with EWOD chips, a custom needle holder was designed and constructed (**Fig. 4A, B**). The holder is designed to position the blunt (delivery) end of the needle at the desired location near the loading edge. In a one-time setup procedure, Cytop®-coated needles are inserted into the holder, rested gently on a 100 µm thick spacer, and fixed in place by tightening screws.

Once this one-time procedure is completed, the pre-assembled fixture is installed onto an EWOD chip by inserting the chip until the loading edge of the cover plate hits the x-direction mechanical stops, followed by tightening the clamping screws such that the top surface of the bottom EWOD substrate contacts the z-direction mechanical stop. The distance d_z of the needle above the substrate surface was sufficient to prevent the needle from damaging the EWOD chip during setup. The fixture can easily and quickly be removed from the chip and reinstalled on a new chip. The holder is designed such that it remains out of the field of view and does not interfere with visualization of the droplets on-chip by microscope or other imaging techniques [25].

4.4 Calibration of Liquid Detector Threshold

A critical parameter is the threshold voltage for liquid detection. The threshold value was determined by first assessing the voltage across the measurement resistor when the loading electrode is activated with no liquid in the chip. This value V_{air} was found to be 7.65 ± 0.01 mV. From our previous work [18], the voltage is expected to linearly increase from V_{air} as the amount of liquid at the loading site is increased. It is desirable that the threshold be as low as possible for liquid detection to represent the smallest possible volume in the sensing region, and that this volume be small compared to the subsequent desired volume delivered by the syringe pump to the chip. For automated applications, a suitable threshold would be several standard deviations above V_{air}, but for the purposes of this paper, a larger threshold of 9.65 mV (i.e. 2.00 mV above V_{air}) was chosen to ensure robust optical detection of liquid presence on the chip. The 2.00 mV above V_{air} threshold corresponded to the volume dispensed by advancing the syringe pump about 2 steps, thus introducing an expected uncertainty of about 4.2 nL in the delivered volume, or about 1% of the total electrode capacity.

The voltage with no liquid in the chip, V_{air}, is likely to vary from chip to chip (due to inconsistencies in the gap height) and from electrode to electrode within the same chip (due to differences in geometry or perhaps parasitic impedances). For most robust operation, it would be advisable to measure V_{air} and its standard deviation at the sensing electrode when the chip is first installed and then compute the threshold based upon this measurement. The measurement of V_{air} can easily be done automatically in software.

4.5 Performance of Liquid Dispensing

To determine performance of volume dispensing, the dispensed droplet volume of MeCN, as measured from CCD images, was compared to the requested volume in the control program (**Fig. 5A**). It can be seen that the dispensed volume is consistent with the desired volume with deviations that are within the error range of volume estimation from CCD images.

As can be seen in **Fig. 5A**, the dispensed MeCN droplets can remain pinned to the edge of the cover plate and the needle tip. Using EWOD force, it is possible to cut the droplet from these features and transport it to another area of the chip for processing or chemical synthesis. Analyzing the volume of these cut droplets (**Fig. 5B**) is more relevant to applications performed on chip. The dispensed volume again varies linearly with the desired volume, but is about ~100 nL smaller than expected. This discrepancy is likely due to loss of MeCN during droplet transport and variability in the cutting point of the droplet from the cover plate edge and needle tip as well as evaporation. It is anticipated that this discrepancy might be a function of liquid properties (surface tension, vapor pressure, etc.) but that the offset could be calibrated for different liquids to obtain accurate dispensed volumes. To reduce evaporation loss, the syringe pump was operated at a high speed setting (600 steps/s = 1260 nL/s) and variations in cutting were minimized by placing the needle as close as possible to the cover plate edge as described earlier.

4.6 Radiosynthesis of [^{18}F]FDG

The system was instrumental in building an automated radiochemical synthesizer for successful production of [^{18}F]FDG on an EWOD chip [10]. Because the tracer is labeled with the short-lived radioisotope fluorine-18, the synthesis must be performed behind radiation shielding. In our previous work, low amounts of radioactive material sufficient for imaging small animals (mice) were synthesized by manually pipetting reagents to the chip. However, scaling up to production of [^{18}F]FDG that would be needed for imaging humans requires a more automated approach to limit radiation exposure during preparation. The chip design and configuration of the dispensing system are illustrated in **Fig. 2A**. The EWOD chip, where the radioactive materials are processed, is located behind a protective radiation shield (constructed from lead bricks) to protect the operator. The computer,

EWOD control system, and syringe pump component of the dispensing system are located outside this shielding. A small hole penetrates the shielding to pass through the tubing from the syringe pump to the needle interface connected to the chip. Separating components that require shielding from those that do not is important as the size, weight, and cost of the system grows rapidly with increase in the size of the shielded components.

The radiochemical synthesis process of [^{18}F]FDG involves an initial azeotropic distillation process consisting of repeated addition of MeCN followed by heating to evaporatively remove trace water prior to the fluorination reaction and thus ensure a high conversion of [^{18}F]fluoride to the intermediate [^{18}F]FTAG. In addition, repeated addition of MeCN droplets is used in several steps to fill up the reaction site and ensure that the full extent of residue/product of a previous step is covered in liquid and thus completely redissolved. Using the automated reagent delivery platform to deliver multiple MeCN droplets enabled rapid and accurate addition of this solvent, and efficient and high-yield synthesis of [^{18}F]FDG on the EWOD chip was achieved (**Fig. 2B**). Other reagents (precursor, HCl, and [^{18}F]fluoride solution) are loaded manually in this demonstration, but could be delivered automatically by replicating the dispensing system and adding appropriate loading sites to the EWOD chip design.

Analysis of the product synthesized on the chip with automated MeCN addition showed faster overall reaction time and high conversion of [^{18}F]fluoride to [^{18}F]FDG consistent with experiments where all reagent deliveries were performed manually. An example radio-TLC chromatogram with conversion of 84.9% is shown in the Supporting Information, **Fig. S2**. This result is comparable to conventional macroscopic methods for synthesizing [^{18}F]FDG [24].

5 Conclusions

We have described a simple but effective system for dispensing a variety of volatile liquids to digital microfluidic chips. The system uses a syringe pump to dispense volumes with high resolution while accuracy is ensured with the use of an extremely sensitive impedance based on-chip liquid detector that enables compensation for evaporation and losses of liquid in the delivery line and chip interface. A special fixture for precisely positioning the needle in relation to the edge of the EWOD chip was designed that can quickly be clamped onto and removed from the EWOD chip. The liquid detection circuit is inexpensive and requires minimal modification to a standard EWOD driving circuit.

Measurement of delivered droplet volume through optical estimation of droplet size combined with accurate measurement of the chip gap (i.e. droplet height) correlated well with a wide range of desired volumes, despite wide variations in time elapsed since a previous droplet was dispensed. As a proof-of-concept demonstration, the dispensing system was integrated with an EWOD chip designed for performing chemical synthesis of radiotracers for medical imaging. Delivery of one reagent was performed with the dispensing system and the performance was found to be comparable to the synthesis performed with all-manual reagent addition. Fully automated droplet dispensing achieved by this platform can address the necessary requirement of shielding and multiple reagent deliveries for on-chip radiopharmaceutical synthesis.

6 Acknowledgements

Funding for this work was provided in part by the Department of Energy (DE-SC0001249, DE-SC0005056), the National Cancer Institute (U54CA151819), and the UCLA Foundation from a donation made by Ralph & Marjorie Crump for the UCLA Crump Institute for Molecular Imaging. The authors thank Nagichettiar Satyamurthy and the staff of the UCLA Biomedical Cyclotron facility for generously providing [^{18}F]fluoride for this work, Dirk Williams and Darin Williams for assistance with design and fabrication of the needle holder and electronic designs and instrumentation help of Robert W. Silverman.

7 References

[1] I. Barbulovic-Nad, S. H. Au, and A. R. Wheeler, "A microfluidic platform for complete mammalian cell culture," *Lab Chip*, vol. 10, no. 12, pp. 1536–1542, Jun. 2010.

[2] D. Bogojevic, M. D. Chamberlain, I. Barbulovic-Nad, and A. R. Wheeler, "A digital microfluidic method for multiplexed cell-based apoptosis assays," *Lab Chip*, vol. 12, no. 3, pp. 627–634, Jan. 2012.

[3] A. R. Wheeler, H. Moon, C. A. Bird, R. R. Ogorzalek Loo, C.-J. Kim, J. A. Loo, and R. L. Garrell, "Digital Microfluidics with In-Line Sample Purification for Proteomics Analyses with MALDI-MS," *Anal. Chem.*, vol. 77, no. 2, pp. 534–540, 2004.

[4] Y.-H. Chang, G.-B. Lee, F.-C. Huang, Y.-Y. Chen, and J.-L. Lin, "Integrated polymerase chain reaction chips utilizing digital microfluidics," *Biomedical Microdevices*, vol. 8, no. 3, pp. 215–225, May 2006.

[5] E. M. Miller and A. R. Wheeler, "A Digital Microfluidic Approach to Homogeneous Enzyme Assays," *Anal. Chem.*, vol. 80, no. 5, pp. 1614–1619, 2008.

[6] R. S. Sista, A. E. Eckhardt, T. Wang, C. Graham, J. L. Rouse, S. M. Norton, V. Srinivasan, M. G. Pollack, A. A. Tolun, D. Bali, D. S. Millington, and V. K. Pamula, "Digital Microfluidic Platform for Multiplexing Enzyme Assays: Implications for Lysosomal Storage Disease Screening in Newborns," *Clinical Chemistry*, vol. 57, no. 10, pp. 1444–1451, Oct. 2011.

[7] Y.-J. Liu, D.-J. Yao, H.-C. Lin, W.-Y. Chang, and H.-Y. Chang, "DNA ligation of ultramicro volume using an EWOD microfluidic system with coplanar electrodes," *Journal of Micromechanics and Microengineering*, vol. 18, no. 4, p. 045017, Apr. 2008.

[8] T. Taniguchi, T. Torii, and T. Higuchi, "Chemical reactions in microdroplets by electrostatic manipulation of droplets in liquid media," *Lab Chip*, vol. 2, no. 1, pp. 19–23, 2002.

[9] G. Marchand, P. Dubois, C. Delattre, F. Vinet, M. Blanchard-Desce, and M. Vaultier, "Organic Synthesis in Soft Wall-Free Microreactors: Real-Time Monitoring of Fluorogenic Reactions," *Analytical Chemistry*, vol. 80, no. 15, pp. 6051–6055, 2008.

[10] P. Y. Keng, S. Chen, H. Ding, S. Sadeghi, G. J. Shah, A. Dooraghi, M. E. Phelps, N. Satyamurthy, A. F. Chatziioannou, C.-J. Kim, and R. M. van Dam, "Micro-chemical synthesis of molecular probes on an electronic microfluidic device," *PNAS*, vol. 109, no. 3, pp. 690–695, 2012.

[11] J. Gong and C.-J. Kim, "All-electronic droplet generation on-chip with real-time feedback control for EWOD digital microfluidics," *Lab Chip*, vol. 8, no. 6, pp. 898–906, 2008.

[12] R. B. Fair, A. Khlystov, T. D. Tailor, V. Ivanov, R. D. Evans, P. B. Griffin, Vijay Srinivasan, V. K. Pamula, M. G. Pollack, and J. Zhou, "Chemical and Biological Applications of Digital-Microfluidic Devices," *IEEE Design & Test of Computers*, vol. 24, no. 1, pp. 10–24, Feb. 2007.

[13] H. Ren, R. B. Fair, and M. G. Pollack, "Automated on-chip droplet dispensing with volume control by electro-wetting actuation and capacitance metering," *Sensors and Actuators B: Chemical*, vol. 98, no. 2–3, pp. 319–327, Mar. 2004.

[14] D. Chatterjee, B. Hetayothin, A. R. Wheeler, D. J. King, and R. L. Garrell, "Droplet-based microfluidics with nonaqueous solvents and solutions," *Lab Chip*, vol. 6, no. 2, pp. 199–206, 2006.

[15] D. Chatterjee, H. Shepherd, and R. L. Garrell, "Electromechanical model for actuating liquids in a two-plate droplet microfluidic device," *Lab on a Chip*, vol. 9, no. 9, p. 1219, 2009.

[16] G. J. Shah, H. Ding, S. Sadeghi, S. Chen, C.-J. Kim, and R. M. van Dam, "Milliliter-to-microliter platform for on-demand loading of aqueous and non-aqueous droplets to digital microfluidics," in *Proceedings of the 16th International Solid-State Sensors, Actuators and Microsystems Conference (TRANSDUCERS)*, 2011, pp. 1260–1263.

[17] S. C. C. Shih, R. Fobel, P. Kumar, and A. R. Wheeler, "A feedback control system for high-fidelity digital microfluidics," *Lab Chip*, 2011.

[18] S. Sadeghi, H. Ding, G. J. Shah, S. Chen, P. Y. Keng, C.-J. Kim, and R. M. van Dam, "On Chip Droplet Characterization: A Practical, High-Sensitivity Measurement of Droplet Impedance in Digital Microfluidics," *Anal. Chem.*, vol. 84, no. 4, pp. 1915–1923, 2012.

[19] M. E. Phelps, "Positron emission tomography provides molecular imaging of biological processes," *PNAS*, vol. 97, no. 16, pp. 9226–9233, Aug. 2000.

[20] W. A. Weber and R. Figlin, "Monitoring Cancer Treatment with PET/CT: Does It Make a Difference?," *J Nucl Med*, vol. 48, no. 1_suppl, p. 36S–44, Jan. 2007.

[21] C. M. Deroose, A. De, A. M. Loening, P. L. Chow, P. Ray, A. F. Chatziioannou, and S. S. Gambhir, "Multimodality Imaging of Tumor Xenografts and Metastases in Mice with Combined Small-Animal PET, Small-Animal CT, and Bioluminescence Imaging," *Journal of Nuclear Medicine*, vol. 48, no. 2, pp. 295 –303, Feb. 2007.

[22] W. A. Weber, "Use of PET for Monitoring Cancer Therapy and for Predicting Outcome," *J Nucl Med*, vol. 46, no. 6, pp. 983–995, Jun. 2005.

[23] P. Salvadori, "POSITRON EMISSION TOMOGRAPHY APPLICATION TO DRUG DEVELOPMENT AND RESEARCH," in *Physics for Medical Imaging Applications*, vol. 240, Y. Lemoigne, A. Caner, and G. Rahal, Eds. Dordrecht: Springer Netherlands, 2007, pp. 341–351.

[24] K. Hamacher, H. H. Coenen, and G. Stöcklin, "Efficient stereospecific synthesis of no-carrier-added 2-[18F]-fluoro-2-deoxy-D-glucose using aminopolyether supported nucleophilic substitution," *J. Nucl. Med.*, vol. 27, no. 2, pp. 235–238, Feb. 1986.

[25] J. S. Cho, R. Taschereau, S. Olma, K. Liu, Y.-C. Chen, C. K.-F. Shen, R. M. van Dam, and A. F. Chatziioannou, "Cerenkov radiation imaging as a method for quantitative measurements of beta particles in a microfluidic chip," *Physics in Medicine and Biology*, vol. 54, no. 22, pp. 6757–6771, 2009.

8 Figures

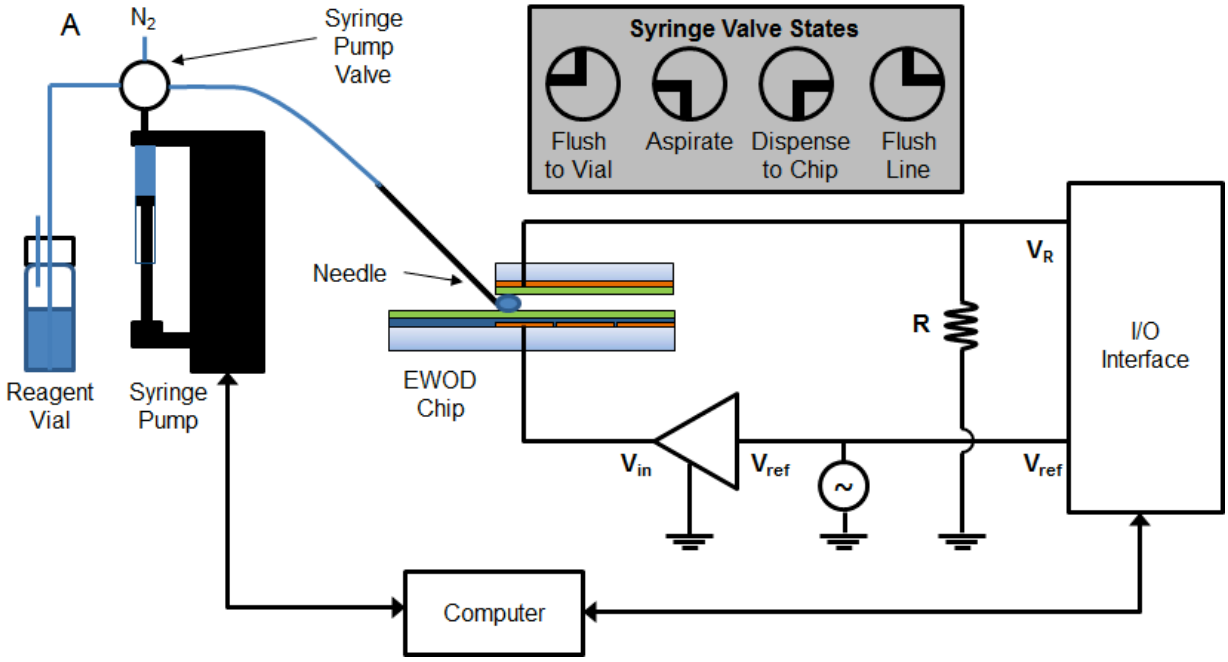

Fig. 1A: (A) Schematic of the reagent dispensing system connected to the EWOD chip

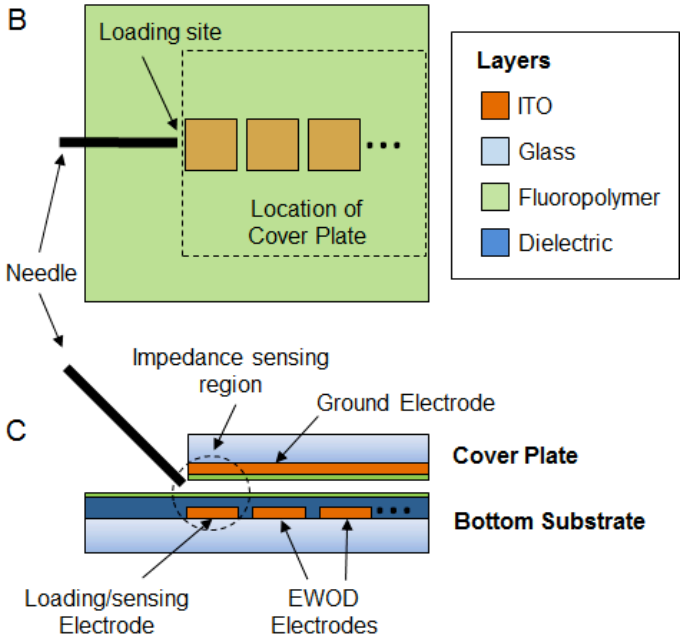

Fig. 1B, C: (B) Top and (C) cross-section view illustrating position of needle for reagent loading.

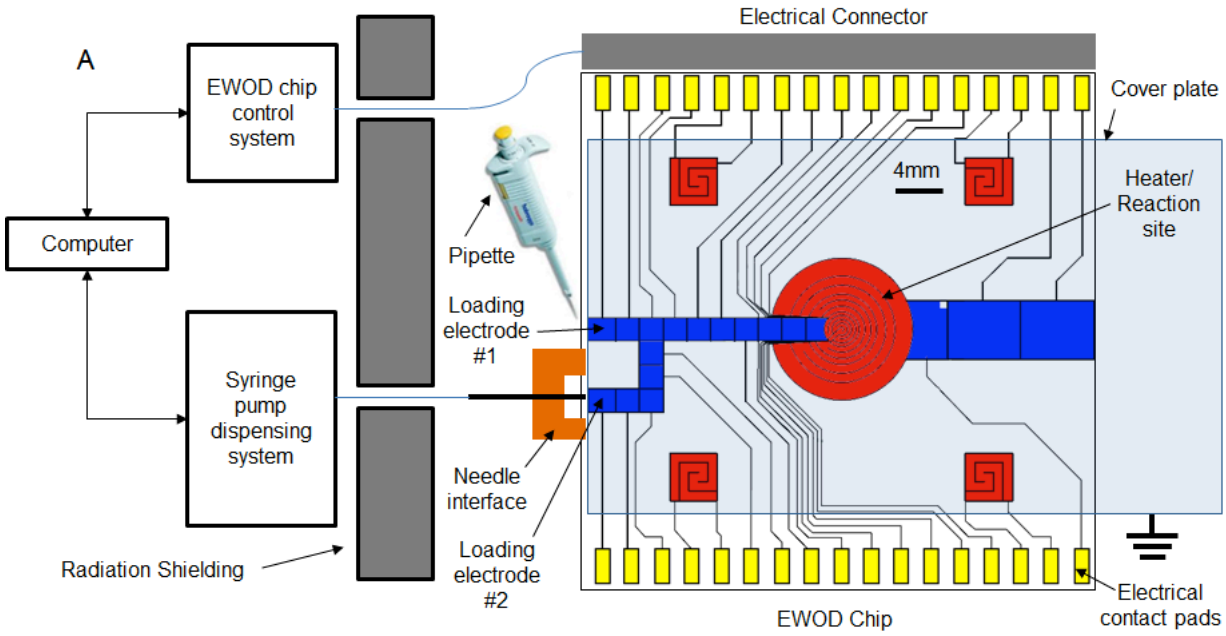

Fig. 2A: (A) Diagram of the system configuration for synthesis of the PET radiotracer [^{18}F]FDG on an EWOD chip. The chip (where radioactive materials are processed) is located behind radiation shielding. Only the needle and holding interface need be located within the shielding. Larger components such as the syringe pump, computer, and EWOD chip control system can be located outside the shielding. In this proof-of-principle demonstration, only one reagent was delivered automatically; the remaining reagents were delivered by pipette.

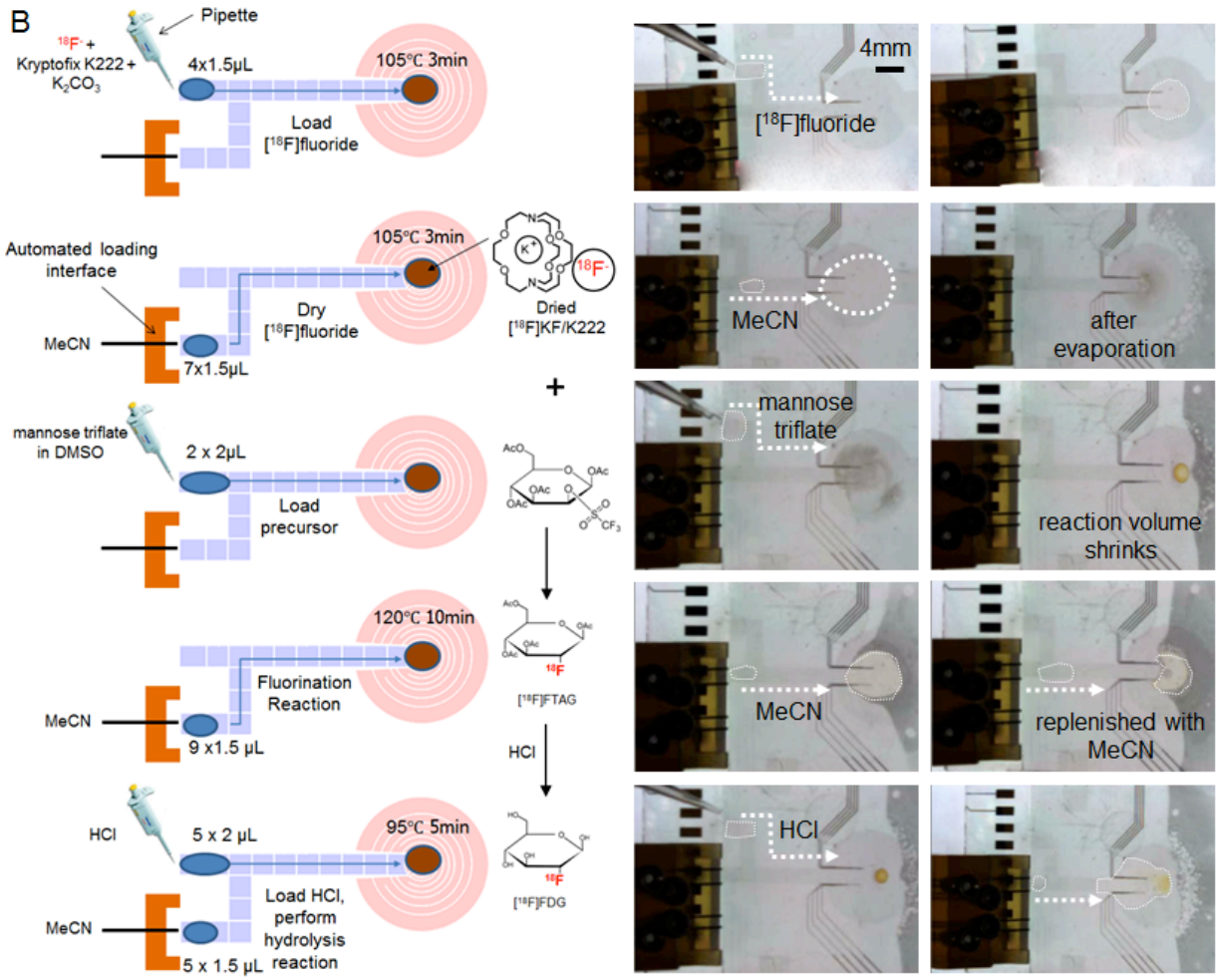

Fig. 2B: (B) [^{18}F]FDG synthesis process. (Left) Schematic of operations and reaction scheme. (Right) Optical micrographs of EWOD chip during the synthesis.

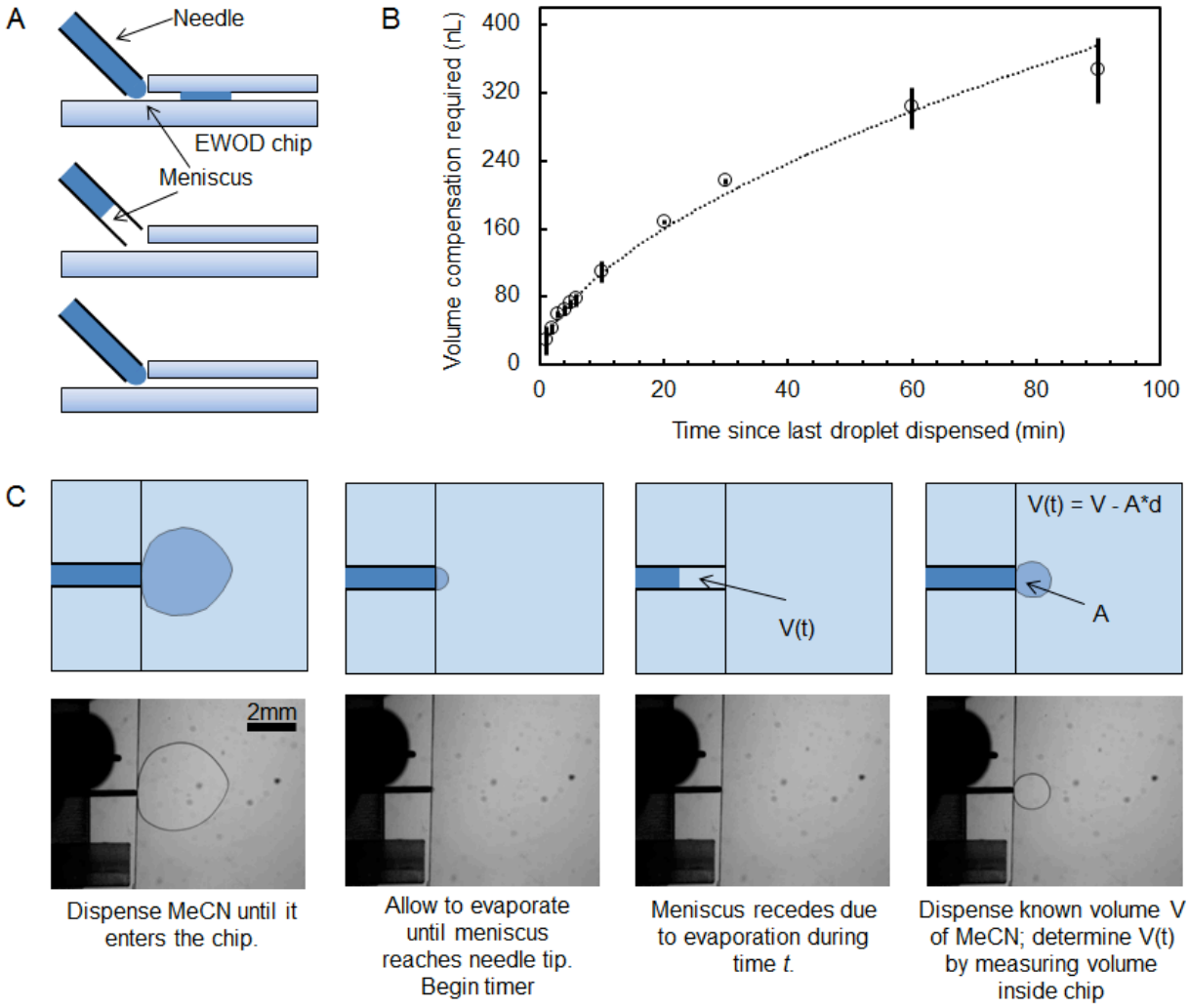

Fig. 3: Dispensing accurate volumes of volatile liquids such as acetonitrile (MeCN) requires compensation for evaporation since the last drop was delivered. (A) Series of schematics showing needle just after dispensing a droplet, meniscus receded due to evaporation during interval before next droplet is demanded, and the meniscus advanced back to the needle tip just prior to dispensing the next droplet. (B) Relationship between the volume compensation required and time elapsed since the last droplet was dispensed. The volume of fluid evaporated is a significant fraction of the nominal droplet size (400 nL for chip designs in this paper) for intervals on the order of 1 min or longer. (C) Experimental procedure for measuring the amount of volume compensation required.

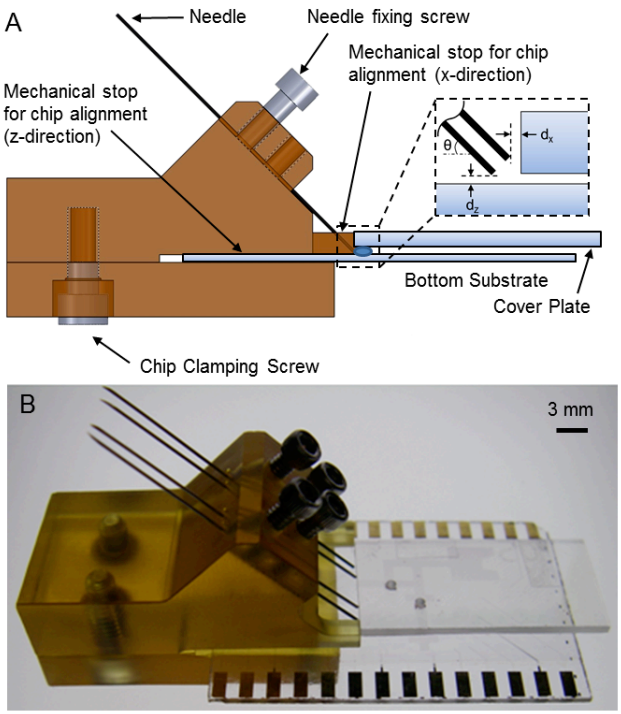

Fig. 4: (A) Design of quick-connect needle holder to rapidly and easily align the needle tips to the EWOD chip In the optimal configuration with θ=45°, d_x≈100µm and d_z≈100µm. (B) Photograph of needle holder assembled with EWOD chip. Only one needle was used for the radiosynthesis demonstration, but the fixture can simultaneously align multiple needles.

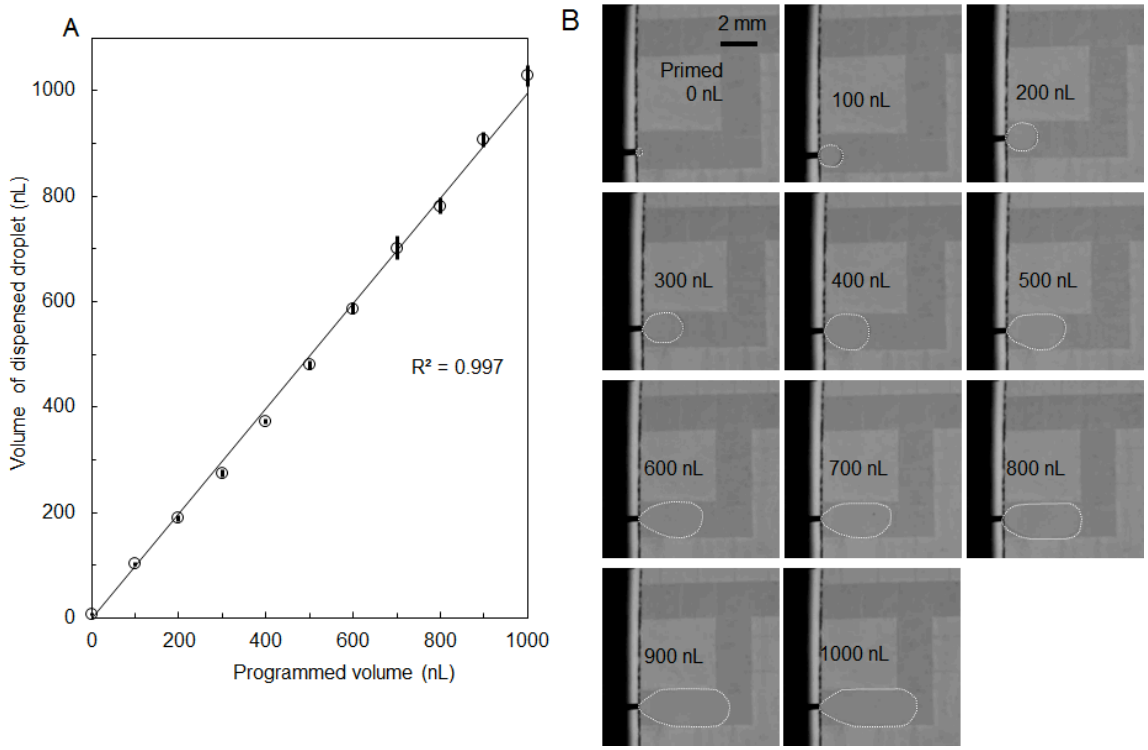

Fig. 5A, B: (A) Comparison of delivered volume of acetonitrile and the volume requested in the software. The dotted line shows the ideal case where the two volumes are equal. The actual delivered volume is determined from the area of the droplet in a CCD image multiplied by the gap height of the EWOD chip. (B) Representative images of delivered droplets for a variety of droplet sizes. Droplets in the images are outlined with a faint white line to enhance visibility. The 0 nL image shows the droplet size in the state immediately after priming (i.e. when the threshold voltage is reached in the liquid detection circuit).

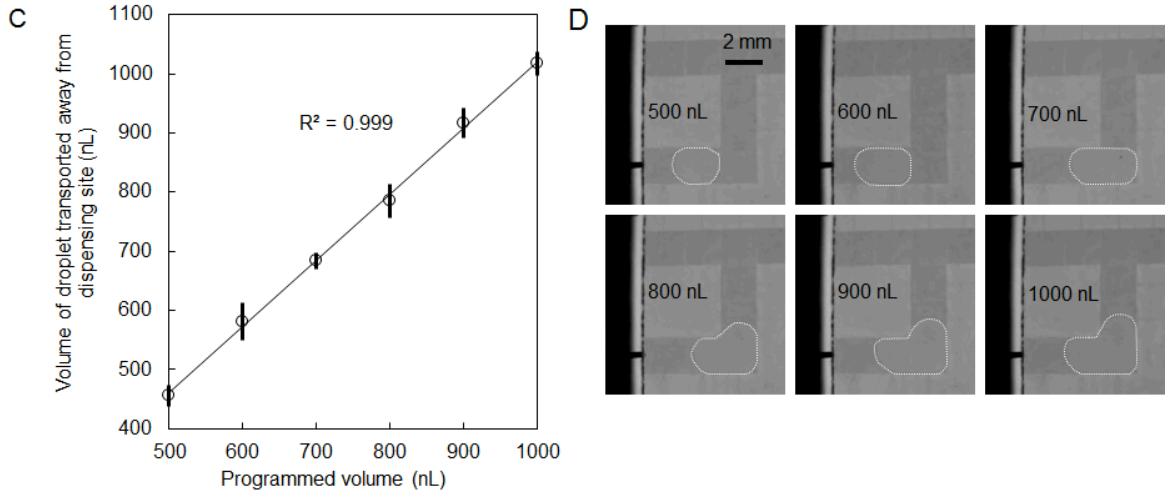

Fig. 5C, D: (C) Comparison of actual volume moved away from the loading electrode by EWOD and the desired volume set in the software. Droplet volumes less than 400 nL were much smaller than the EWOD electrodes and could not be transported away from the loading electrode. (D) CCD images of the dispensed droplet are outlined in faint white lines. Actual volume was determined from the area of the droplet multiplied by the gap height in the chip.